Rossini

RObot enhanced SenSing, INtelligence and actuation to Improve productivity and job quality in manufacturing

Deliverable

D7.1 Collision test results

Deliverable Lead: Fraunhofer IFF

Deliverable due date: 30/09/2020 (M24)

Actual submission date: 30/09/2020

Version: V1.0

This project receives funding in the European Commission's Horizon 2020 Research Programme under Grant Agreement Number 818087

Document Control Page	
Title	D7.1 Collision Test Result
Creator	Fraunhofer IFF
Description	Collision test results to validate a new technique for the model-based evaluation of transient human-robot contacts
Contributors	Fraunhofer IFF
Creation date	28/09/2020
Type	Report
Language	English
Audience	☒ public ☐ confidential
Review status	☐ Draft ☐ WP leader accepted ☒ Coordinator accepted
Action requested	☐ to be revised by Partners ☐ for approval by the WP leader ☐ for approval by the Project Coordinator ☒ for acknowledgement by Partners

Version	Author(s)	Changes	Date
0.0	Herbster, Sebastian; Behrens, Roland (Fraunhofer IFF)	Initial Version of Document	25/09/2020
1.0	Herbster, Sebastian; Behrens, Roland (Fraunhofer IFF)	Final Version of Document	30/09/2020

Table of Contents

Table of Contents 1
Abstract 3
Scope 4
List of Acronyms 5
List of Figures 5
List of Tables 5
1 Introduction 6
2 Technical Approach 6
3 Model Based Results 7
4 Experiments 8
5 Experimental Results 10
6 Discussion 11
6.1 Error Analysis 11
6.2 Simplification of the conversion technique 13
7 Summary 14
8 Conclusion and Outlook 15
Acknowledgment 16
Annex: Collision test results for different configurations 17
9 References 25

Disclaimer

Abstract

With the increasing importance of collaborative robots in industrial manufacturing, their economic efficiency is becoming more and more important. Today, one approach to prevent collaborative robots from injuring humans is to assure that the robot does not exceed biomechanical limits in the event of an accidental contact such as collisions or clamping. The ability of the robot to avoid collision forces beyond the limits must be validated with a biofidelic pressure and force measurement device (PFMD) that mimics the biomechanical characteristics of the human body.

The proper use of the PFMD requires to mount it on a rigid structure. Consequently, the test setup is solely capable to simulate the dynamics and biomechanical response of a quasi-static contact in which the human body part cannot move during the collision. In contrast, the affected human body part can freely move in transient contact. Since such contact transfer a part of the impact energy into kinetic energy stored in the moving body part, the contact forces are significantly lower as they are in quasi-static contact with the same amount of impact energy. However, measuring transient contacts in a reliable manner is not possible due to the constraint to fix the PFMD for the test. A direct consequence of this is that cobots must move slower than they could in order to ensure in the measurement they comply with the limits.

This deliverable presents a technique that transfers the results from measurements taken with a fixed PFMD into results taken with a free moving PFMD of a specific mass. The technique utilizes a model-based conversion. Findings from experiments with three different cobots confirmed that the conversion technique has a considerable accuracy and allows to increase the moving velocity of cobots without compromising their ability to mitigate the risk of injury to humans. Therefore, the conversion technique has great potential to increase the average productivity of cobots.

Scope

In WP7.1 Fraunhofer IFF develops a new technique for evaluating transient human-robot contact (i.e., free collisions / impacts). The input parameters of this technique are the mass of the human body and robot that appear to be effective at the point of impact. To calculate the apparent mass of the human, Fraunhofer IFF created a multi-body system that comprises an accurate mass distribution, arrangement of joints, and limb lengths. The determination of the apparent robot mass does not require a model. Thanks to the mandatory validation of the robot through measurement, the apparent robot mass can be estimated from the force recorded. With having both parameters in place, the conversion technique presented here provides a factor that scales down the maximum contact force measured by a fixed PFMD and leading ultimately to the maximum force of the transient contact that cannot be measured due to technical constraints of the PFMDs used today.

List of Acronyms

European Commission	EC
Cobot	Collaborative robot
Pressure and Force Measurement Device	PFMD

List of Figures

Figure 1: Simulation and conversion model of a fixed and free PFMD 7
Figure 2: Result of the simulated impact force compared to the predicted force of the conversion method for an UR10e robot with a payload of 66% 8
Figure 3: Experimental test-setup for measuring the impact force of a collaborative robot with a freely moving PFMD 9
Figure 4: Comparison of maximum forces from tests with a fixed and moveable PFMD with those obtained with the conversion technique 10
Figure 5: Sensitivity analysis of the conversion with respect to the input parameters human mass and apparent mass of the robot 11
Figure 6: Sensitivity of the apparent robot mass with respect to the input parameters velocity and momentum 12
Figure 7: Distribution of the relative and absolute error of the conversion technique (the red line indicates 100% accuracy; each error on the left hand-side of the red line indicates that the conversion technique yields conservative and, thus, safer results) 13
Figure 8: Approximation of the momentum using the area of a triangle 14
Figure 9: Comparison of measured and converted impact force for all configurations according to Table 3 (~1000 data points) using $\boldsymbol{papp}$ to calculate $\boldsymbol{mR}*$ 14
Figure 10: Results from experimental tests and obtained with both conversion techniques 15

List of Tables

Table 1: Characteristics of the biofidelic PFMDs used for the experimental validation 8
Table 2: Joint configurations of the robots at the impact position 9
Table 3: Test configurations of the different robots 9

1 Introduction

In the closest form of human-robot collaboration, robots and humans complete common tasks next to each other at the same time (Behrens et al. 2015). At such workplaces, accidental contacts such as clamping or collisions constitute a risk of injury to human that technical measures cannot eliminate entirely, since there is always the possibility of a technical failure or foreseeable misuse. As a metric and reference for acceptable risks, ISO/TS 15066 defines biomechanical force and pressure limits for multiple body parts. The technical risk-mitigation measures of the robot must reliability prevent it from exceeding these limits.

To prove this, the robot operator must simulate the foreseen accidental contacts and measure the maximum forces and pressures using a so-called biofidelic Pressure and Force Measurement Device (PFMD). A proper PFMD consists of bumper covered by a soft damping material and a mechanical spring. The spring carries the bumper and transmits the contact force to a load cell. The combination of spring and damping material enables the PFMD to mimic the viscos-elastic characteristic of a specific body location. Altogether, ISO/TS 15066 distinguishes between 29 body locations. Each of them corresponds to a specific spring-damper combination (Huelke und Ottersbach 2012).

During the validation measurement, the velocity of the robot must be reduced until the measured contact forces and pressures do not exceed the applicable limits (BGHM 2017). The proper use of the PFMD requires to mount it on a rigid structure that avoids any undesired displacements of the PFMD. This requirement, however, does not reflect the conditions of a free and truly transient contact, in which the human body part hit by the robot can move freely.

Falco et al. (2012) and Oberer-Treitz (2017) presented moveable PFMDs that are capable of simulating the dynamics of free collisions. They attached a PFMD to a linear guide rail and adhered additional weight to it, so that the total mass of the movable parts reflect exactly the mass of the human body part under test. The US American de-facto standard RIA T R15.806-2018 incorporated the concept of a free-moving PFMD and specifies that it should be used to evaluate free collisions instead of a fixed PFMD. A movable PFMD has, however, the essential limitation that it can only measure collisions within the horizontal plane.

Within the ROSSINI project, the Fraunhofer IFF develops a technique that allows to convert the results recorded with a fixed PFMD into results that reflect the results taken with a free-moving PFMD. This deliverable reports on the experiments that Fraunhofer IFF has executed to evaluate the accuracy and reliability of the conversion technique through experiments with two different PFMDs and three collaborative robots (UR3e, UR10e, Doosan M0607).

2 Technical Approach

The development of the proposed conversion technique can be shown by the analysis of an accurate and simplified impact model. The accurate model in Figure 1 (top) reproduces the impact behavior of a compliant robot that collides with a biofidelic PFMD. For such a constellation, it is possible to consider the compliant robot as a two-mass oscillator (Bicchi und Tonietti 2004; Haddadin et al. 2012). The first mass represents the contribution of the robot joints m_D and the second m_L the contribution of the robot links, while c_T is the elasticity that connect joint drives and links. The other part of the model covers the PFMD. The parameters c_D and d_D factor in the damping and elasticity of the soft material on the PFMD's bumper with total mass m_B. A mechanical spring with stiffness c_S absorbs the impact energy from the bumper and transmits the force generated to a load cell. Variable F_I denotes the impact force measured by the load cell. A high reliability and a robust setup necessitates to prevent the PFMD from moving during the measurement. However, testing transient contacts like free collisions require a device that can move in the direction of the contact force. Moreover, the total mass of the device must precisely correspond to the mass of the human body part m_H.

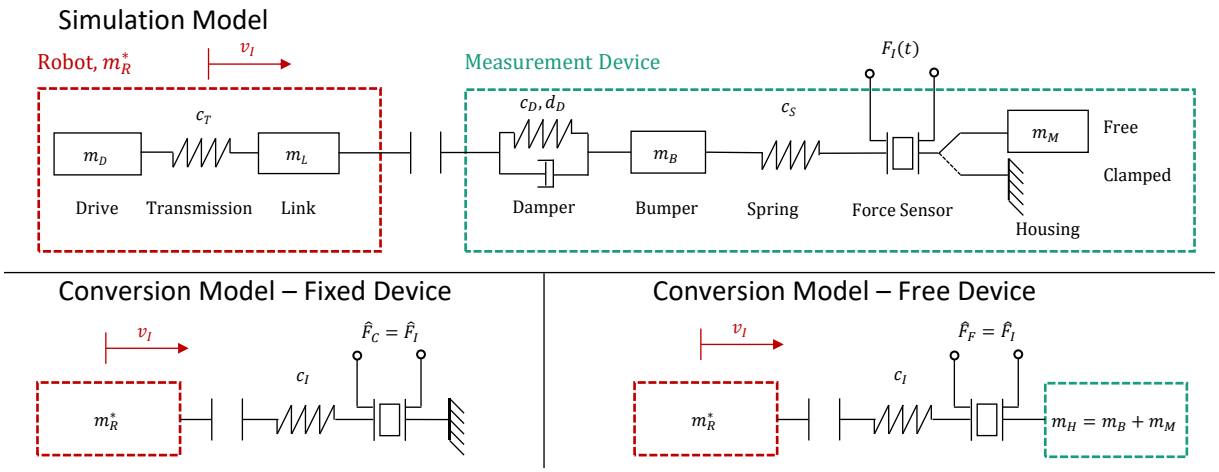

Figure 1: Simulation and conversion model of a fixed and free PFMD

To convert the maximum contact force $\hat{F}_C$ from a fixed PFMD into the maximum contact force $\hat{F}_F$ of a movable PFMD, the complexity of the simulation model must be reduced, ultimately leading to the model shown Figure 1 (bottom). This model assumes that m_D, m_L, and c_T are included in an apparent robot mass m_R^*. Due to its simplified structure, the comparison of the energies stored in elasticities and masses of both devices (fixed and free) lead to the following desired conversion technique

$$\hat{F}_F = \hat{F}_C \sqrt{\frac{m_H}{m_H + m_R^*}} \quad . \tag{2.1}$$

The expression reflects the relative difference between the maximum force of a free $\hat{F}_F$ and a clamped collision $\hat{F}_C$. Unlike m_H, the apparent robot mass m_R^* is unknown, but can be estimated with the momentum of the impact

$$p = m_R^* \, v = \int_{t_0}^{t_{max}} F_C(t) \, dt \quad , \tag{2.2}$$

where v is the impact velocity, t_0 the time of initial contact, and t_{max} the time at which the impact force $F_C(t)$ recorded over time reaches $\hat{F}_C$.

3 Model Based Results

A simulation with the accurate model (Figure 1, on the top) was executed to study the conversion technique. The model parameters applied were precisely adjusted to the robot and PFMD that we later used in the experimental tests for model validation. The robot masses m_L and m_D have been calculated with the method presented by Khatib (1987, 1995). This method projects the mass matrix of the robot manipulator $\mathbf{M}^+$ (incl. the contribution of drives and links) to a directional point mass m_R that equals the sum of m_L and m_D

$$m_R = m_L + m_D \quad . \tag{3.1}$$

Here, m_L denotes the directional point mass that can be calculated with the mass matrix $\mathbf{M}$, which does not contain contributions from the joint inertias. Then, m_D can easily be calculated by subtracting m_L from m_R. The robot's effective stiffness c_T was obtained in a similar same way, but based on the stiffness matrix $\mathbf{K}_q$ instead of $\mathbf{M}$ (Zinn et al. 2004; A. Albu-Schaffer et al. 2004).

The compliant configuration of the PFMD used for the simulation corresponded to the back of the hand (ID 25 in ISO/TS 15066). A spring of 75 N/mm combined with a adhering a damping material of shore hardness 70 simulates the biomechanical characteristics of this specific body part (BGHM 2017). Both stiffness parameters, i.e. c_D for the damping material and c_S for the spring, were measured beforehand with a testing system and the same impactors that were used in the experiments. The damping parameter d_D was estimated in impact experiments at various collision speeds.

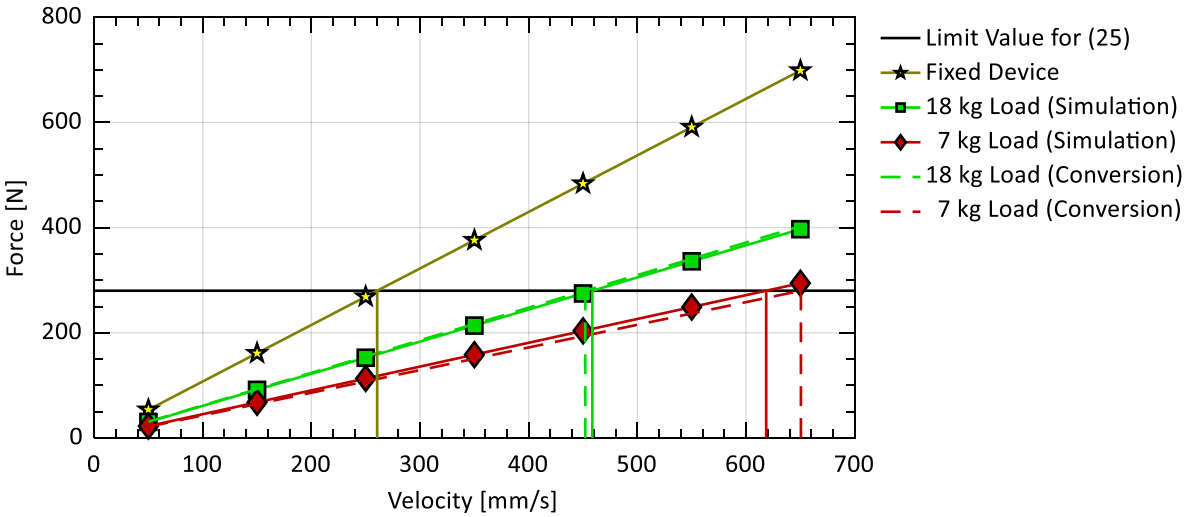

Figure 2: Result of the simulated impact force compared to the predicted force of the conversion method for an UR10e robot with a payload of 66%

Figure 2 shows the impact force over impact velocity obtained from the simulation with a PFMD for fixed and free conditions. The solid line in yellow indicates the results for the fixed PFMD. The results for the free PFMD (solid lines with boxes and diamonds in green and red for 7 kg and 18 kg) clearly show that the impact forces decreases when m_H decreases. The dashed lines are the results obtained with the conversion technique Eq. (2.1) that converts the forces $\hat{F}_C$ of the fixed case (represented by the solid line in yellow) into the forces $\hat{F}_F$ for the free case (represented by the dashed lines in green and red). For both masses, the curves confirm a good match between the results from the simulation with the free PFMD and the ones obtained from the conversion of the results from the simulation with the fixed PFMD. The intersection points of all lines with the dark vertical lines indicate the maximum allowable robot velocity when assuming a force limit of 280 N (here: back of the hand). In case of the fixed PFMD the maximum allowable robot velocity would be 261 mm/s. This result would be the one obtained in a test with a properly used PFMD. According to the simulation of a free collision with a body part of 18 kg (which is far beyond the expected weight of an outreached hand), the maximum allowable speed will be 76% higher compared to the speed that can be considered as safe when working with a fixed PFMD. For the same configuration, the conversion technique estimates an increase of 74%. The considerable low difference between both results demonstrates that the proposed conversion techniques obtains sufficiently accurate results. To ensure that this accuracy can also be achieved in real collision tests, experiments with three robot were carried out in a lab environment.

4 Experiments

As the analysis of the simulation data has shown, the mass of the free moving PFMD affects the maximum impact force significantly. Therefore, it was necessary to gather results from collision experiments with a freely moving PFMD of different total masses. Figure 3 shows the test setup that Fraunhofer IFF has developed for the experiment. It bases on the concept of a freely movable PFMD as illustrated in RIA T R15.806-2018.

The test setup consists of one of the three collaborative robot (UR3e, UR10e, Doosan M0607) that was equipped with a cylindrical impactor of 50 mm in diameter as a tool simulant. Additional weights were mounted on the tool to adjust the payload up to the allowable maximum. The PFMD was sitting on a movable carrier on low-friction linear guides (static friction force was approximately 2 N). A large industrial robot was used to hold the assembly consisting of guides and the PFMD under test. For the measurement of the impact force, two different PFMDs with a similar design were used as listed in Table 1.

Table 1: Characteristics of the biofidelic PFMDs used for the experimental validation

Name	Manufacturer	Force Range [N]	Sampling Frequency [kHz]
PRMS	PILZ	0…500	2
KOLROBOT	IFA	0…1000	10

In the test with free collisions, the total mass of the freely moving PFMD ranged from 4 to 22 kg (see Table 3). The simulation of quasi-static collisions required to connect the movable carrier with the system's ground plate, so that any movement along the guides was disabled. Each robot was tested with the joint configuration listed in Table 2.

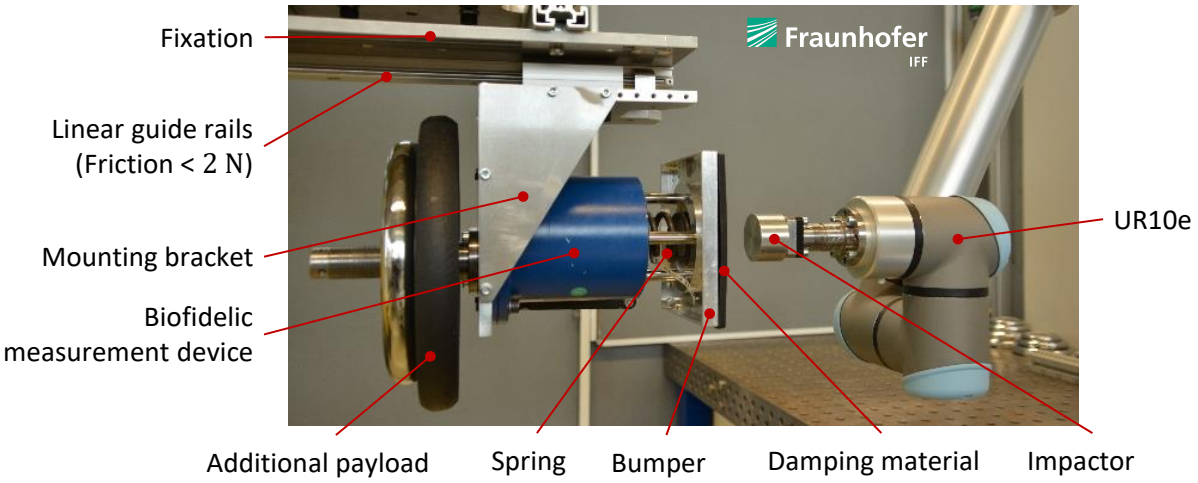

Figure 3: Experimental test-setup for measuring the impact force of a collaborative robot with a freely moving PFMD

The validation experiments had the objective to ensure that the conversion technique obtains accurate results for any given combination of damping material and spring. Therefore, every test was executed with combinations that correspond to three different body parts, namely the Abdomen (10), the Sternum (8) and the Back of the Hand (25). Moreover, it was desired through the tests to exclude any negative influences of the robot's payload on accuracy of the conversion technique. Therefore, the tests with the UR10e were executed with three different payloads. Altogether, the test plan of the experiments includes 120 combinations, whereas every combination required to be measured ten times in average.

Table 2: Joint configurations of the robots at the impact position

	A1 [°]	A2 [°]	A3 [°]	A4 [°]	A5 [°]	A6 [°]
UR3e	-90	-120	-126	247	-90	0
UR10e	-90	-120	-126	67	90	0
Doosan M0607	0	-45	-90	0	45	0

Table 3: Test configurations of the different robots

	UR3e	UR10e	Doosan M0607
Payload Robot [kg]	2,1	3,6; 6,9; 10,2	0,6
Payload Robot [%]	70	36; 69; 102	10
Force Threshold for Safety Stop [N]	50	100	50
Velocity of the robot [mm/s]	50…450	50…650	50…650
PFMD	IFA KOLROBOT	IFA KOLROBOT PILZ PRMS	IFA KOLROBOT
Mass of free PFMD [kg]	IFA KOLROBOT: 6; 12; 17; 22 PILZ PRMS: 4; 10; 15; 20		
Biofidelic Combination	Abdomen (10): Spring: 10 N/mm; Damper: SH10 Sternum (8): Spring: 25 N/mm; Damper: SH70 Back of the hand (25): Spring: 75 N/mm; Damper: SH70		

During the experiments, the robot executes a linear movement at different velocities (starting from 50 and increasing to 650 mm/s) perpendicular towards the PFMD. The starting position of the path was far enough from the impact position and, thus, assured that the robot could reach the desired velocity before colliding with the PFMD. The safety functions of the robot monitored the external forces acting on the robot. They forced

the robot to execute an emergency stop if the magnitude of these forces exceeded the smallest threshold that the robot controller could detect (see Table 3).

5 Experimental Results

The following analysis of the experimental results compares the maximum impact forces measured in transient collisions with a moveable PFMD with those that were obtained from quasi-static collisions with a fixed and afterwards converted with technique presented above. The apparent robot mass m_R^* was estimated from the impact forces recorded by the fixed PFMD using Eq. (2.2). The mass of the human body part m_H was considered as given. Additional weights were used to adjust the total mass of the freely moving PFMD exactly to m_H.

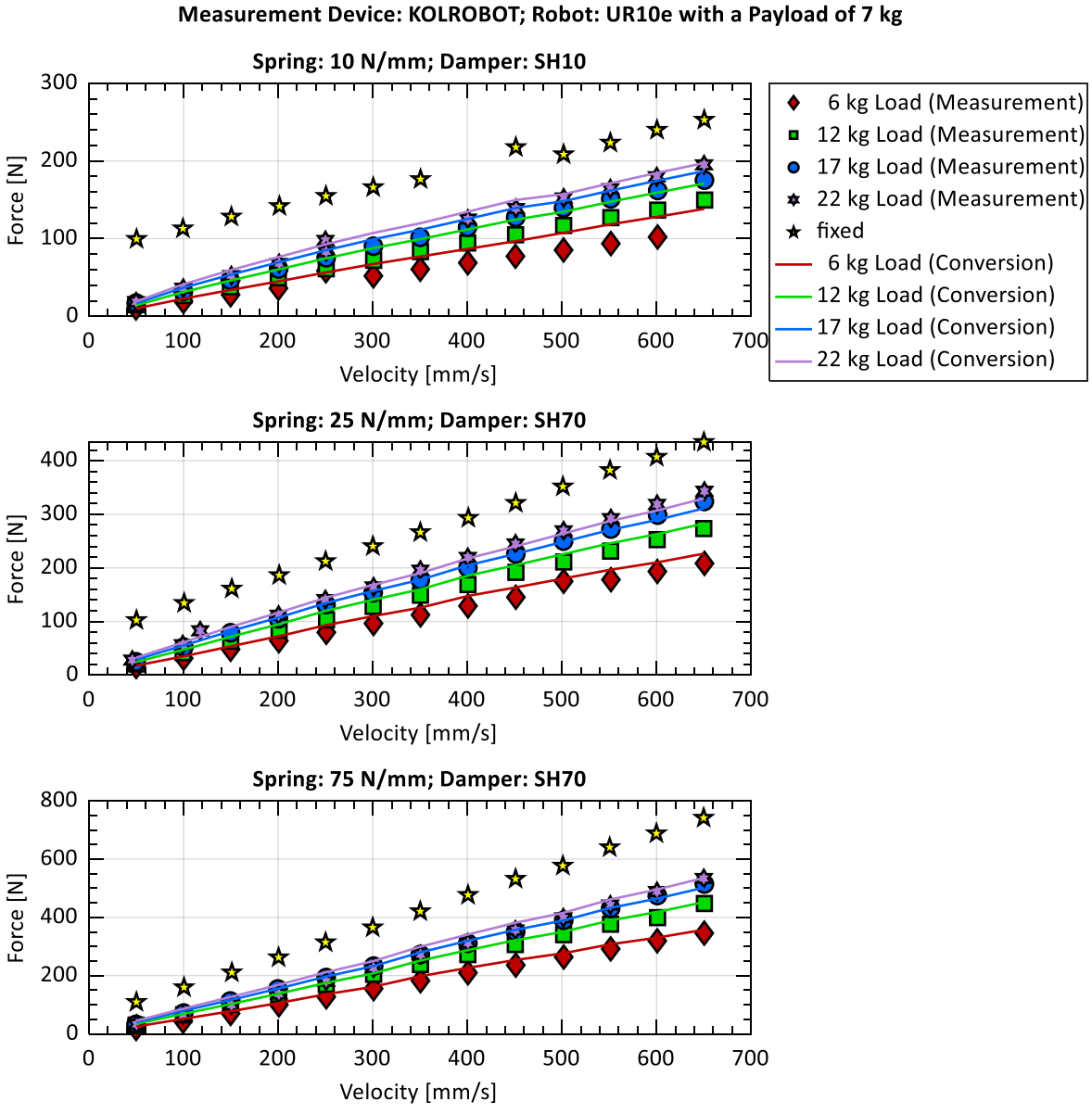

Figure 4: Comparison of maximum forces from tests with a fixed and moveable PFMD with those obtained with the conversion technique

Figure 4 shows one sample of the experimental results obtained (more results are given in Annex A). Each of the three diagrams contains the result measured with a different configurations of the PFMD under examination. The markers in the diagram indicate single measurement results from tests with the fixed and moveable PFMD. The solid lines are the result obtained with the conversion technique, which are based on the measurement values of the fixed PFMD. It is clearly visible that the impact force increases linearly over the impact velocity. Obviously, the linear course is not compromised by the spring-damper configuration used for

the PFMD as already confirmed shown by the simulations executed with the models of Section 3. Moreover, it can be clearly seen that the impact forces from the tests with the moveable PFMD are significantly lower than those of a fixed PFMD. This effect is getting stronger when decreasing the total mass of the human body. And finally, the forces obtained with the conversion technique are slightly higher as those measured with the movable PFMD. In general, it can be concluded that the conversion technique achieves almost the same accuracy for results from experimental tests as it did for results from simulations.

6 Discussion

6.1 Error Analysis

A sensitivity analysis regarding the input parameters of the conversion technique is performed to study the influences of uncertainties on the overall accuracy. Of particular interest is the following part of Eq. (2.1)

$$c = \sqrt{\frac{m_H}{m_H + m_R^*}} \tag{6.1}$$

that calculates a factor < 1 to convert $\hat{F}_C$ into $\hat{F}_F$. To determine the sensitivity with respect to the input parameters the partial derivatives for m_H and m_R^* must be calculated

$$\begin{aligned} \frac{\partial c}{\partial m_H} &= \frac{m_R^*}{2(m_H + m_R^*)^2 \sqrt{\frac{m_H}{m_H + m_R^*}}} \\ \frac{\partial c}{\partial m_R^*} &= -\frac{m_H}{2(m_H + m_R^*)^2 \sqrt{\frac{m_H}{m_H + m_R^*}}} \quad . \end{aligned} \tag{6.2}$$

The summation of the partial derivatives gives the total error

$$\Delta c = \frac{\partial c}{\partial m_H} \Delta m_H + \frac{\partial c}{\partial m_R^*} \Delta m_R^* \quad . \tag{6.3}$$

Figure 5 shows the courses of sensitivity for each parameter. It indicates that the collision masses m_H and m_R^* have a non-linear effect on the conversion result. The absolute magnitude of the sensitivity for m_H and m_R^* decreases with increasing mass. However, the sensitivity of m_R^* with respect to c is negative, meaning that an underestimation of m_R^* will result in a higher scaling factor or higher impact force ($\Delta m_R^* < 0$ leads to $\Delta c > 0$ and then to $\Delta \hat{F}_F > 0$).

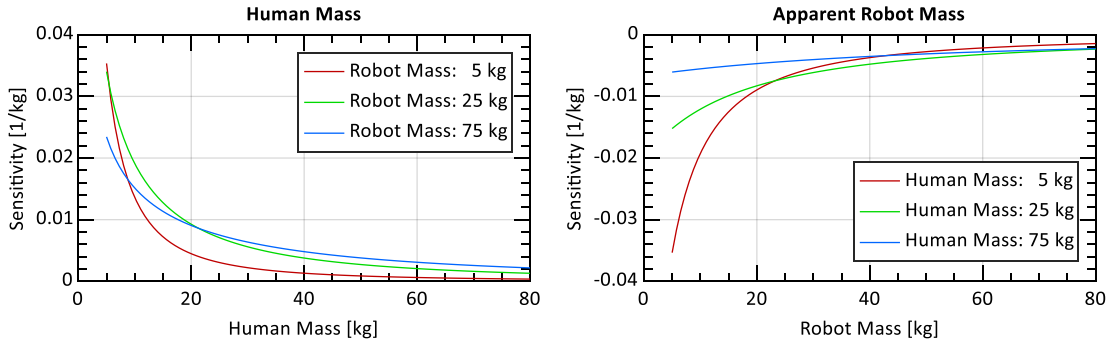

Figure 5: Sensitivity analysis of the conversion with respect to the input parameters human mass and apparent mass of the robot

Since m_H is assumed to be given, the estimation of m_R^* must be analyzed in more depth. The partial derivatives of Eq. (2.2) with respect to the input parameters momentum p and impact velocity v are

$$\frac{\partial m_R^*}{\partial v} = -\frac{p}{v^2}$$
$$\frac{\partial m_R^*}{\partial p} = \frac{1}{v} \tag{6.4}$$

that further give the following expression for the total error

$$\Delta m_R^* = \frac{\partial m_R^*}{\partial v}\Delta v + \frac{\partial m_R^*}{\partial p}\Delta p \quad . \tag{6.5}$$

Eq. (6.4) **Error! Reference source not found.**indicates a proportional influence of p and a non-linear negative one of v on Δm_R^*, which causes m_R^* to decrease in case Δv is positive. Figure 6 gives a detailed insight. The absolute magnitude of the sensitivity of m_R^* decreases with increasing v. This behavior indicates that the estimation accuracy is better the higher the velocities.

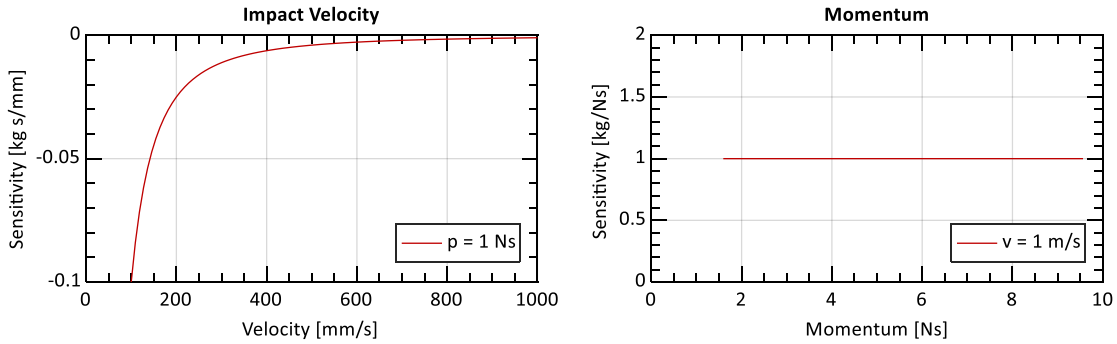

Figure 6: Sensitivity of the apparent robot mass with respect to the input parameters velocity and momentum

To study whether the sensitivity has significant influence on the conversion technique, the following relative error is introduced

$$\Delta x_{rel} = \frac{\hat{F}_{conv}}{\hat{F}_{meas}} - 1 \quad . \tag{6.6}$$

The correspond absolute error is

$$\Delta x_{abs} = \hat{F}_{conv} - \hat{F}_{meas} \quad . \tag{6.7}$$

Both can be calculated from the converted froce $\hat{F}_{conv}$, obtained with the conversion technique, and the impact force $\hat{F}_{meas}$ measured with a movable PFMD. Figure 7 shows the distribution of the errors in a histogram. It includes all samples from the experimental tests, which incorporate more than 1.000 individual results. The error distribution shows that 90% of the impact forces obtained with the conversion technique exceed the forces measured in tests with the moveable PFMD. The mean errors are $\Delta\bar{x}_{rel} = 13\%$ and $\Delta\bar{x}_{abs} = 12$ N. Given this tendency, it can be concluded that the conversion technique yields slightly higher impact forces. Consequently, the conversion technique can be considered to be conservative as higher forces ultimately result in lower but safer robot velocities.

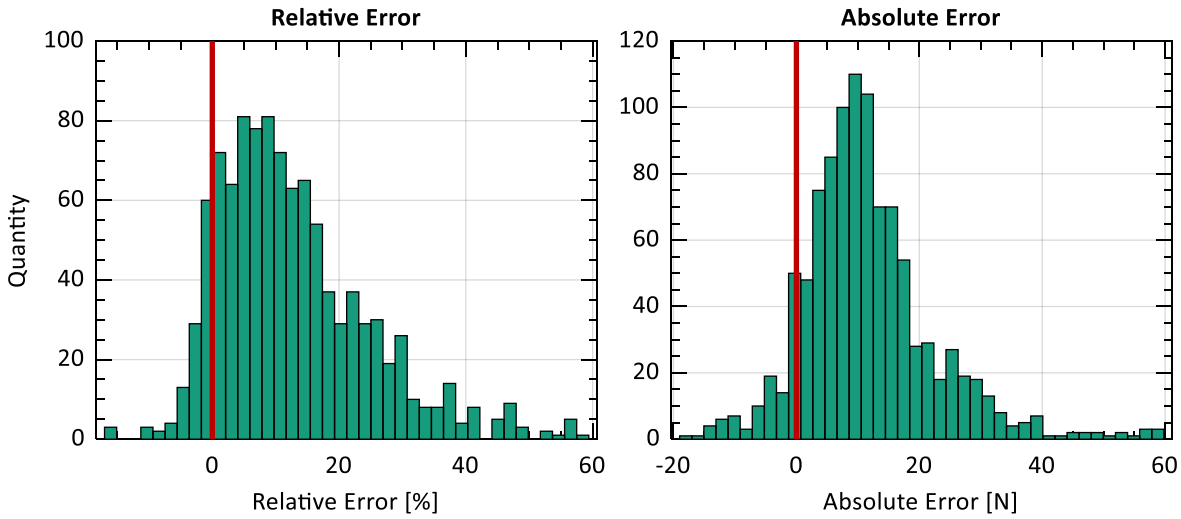

Figure 7: Distribution of the relative and absolute error of the conversion technique (the red line indicates 100% accuracy; each error on the right hand-side of the red line indicates that the conversion technique yields conservative and, thus, safer results)

The error histograms confirm that the parameters with a positive influence on the estimation of the impact force dominate. Since $\hat{F}_C$ and m_H can be considered as accurate or given, the conservative tendency of the converted values must be caused by an systematic underestimation of m_R^*. That means that the technique to estimate m_R^* delivers basically too small values, which possibly results from $\Delta v > 0$ or $\Delta p < 0$ as one can derive from Eq. (6.4). We assume that the calculation of p tends to yield smaller values, since the exact time of initial contact t_0 is difficult to detect. Given this result, it must be highlighted that the conversion technique can underestimate the impact forces, even though the probability for this is low.

6.2 Simplification of the conversion technique

The error analysis has shown that underestimations of p lead to conservative estimates and lower robot velocities. This finding can be used to further simplify the estimation of the apparent robot mass m_R^*. Especially for end-users who do not have direct access to the measurement data or the knowledge to apply Eq. (2.2), it might be difficult to obtain p. An approximation of the integral can be obtained when considering p as the area of a triangle

$$p_{app} = \frac{1}{2}(t_{max} - t_0)\hat{F}_C \ , \tag{6.8}$$

where $\hat{F}_C$ is the maximum contact force at time t_{max}. Figure 8 compares the triangle approximation to the exact integral. The area of the triangle corresponds to a slightly smaller momentum p. According to Eq. (6.4), a negative momentum error $\Delta p < 0$ leads to an underestimation of m_R^* and ultimately to higher collision forces $\hat{F}_F$ (see Eq. (6.2)) and, consequently, to lower, but sill acceptable and safe robots velocities.

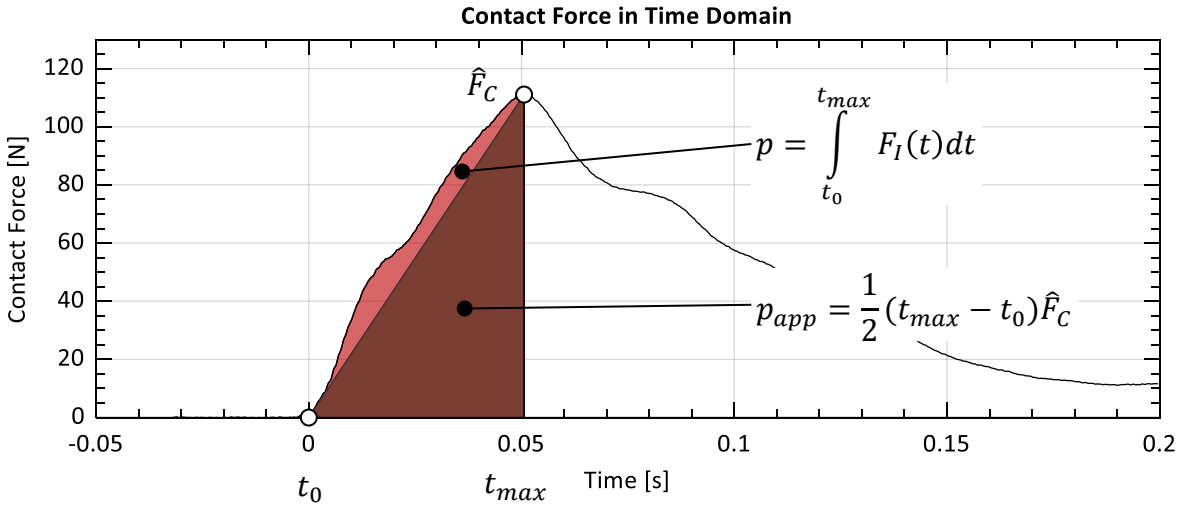

Figure 8: Approximation of the momentum using the area of a triangle

The simplified conversion technique that considers p as the area of a triangle was applied to all experiment results using Eq. (6.8) to calculate m_R^*. The errors compared to the measurements from the tests with the movable PFMDs are shown in Figure 9. As expected, the simplified conversion technique delivers a higher relative $\Delta\bar{x}_{rel} = 15\%$ and absolute mean error $\Delta\bar{x}_{abs} = 13$ N, whereas the shape of the error distribution remains almost identical (result with exact integral: $\Delta\bar{x}_{rel} = 13\%$, $\Delta\bar{x}_{abs} = 12$ N).

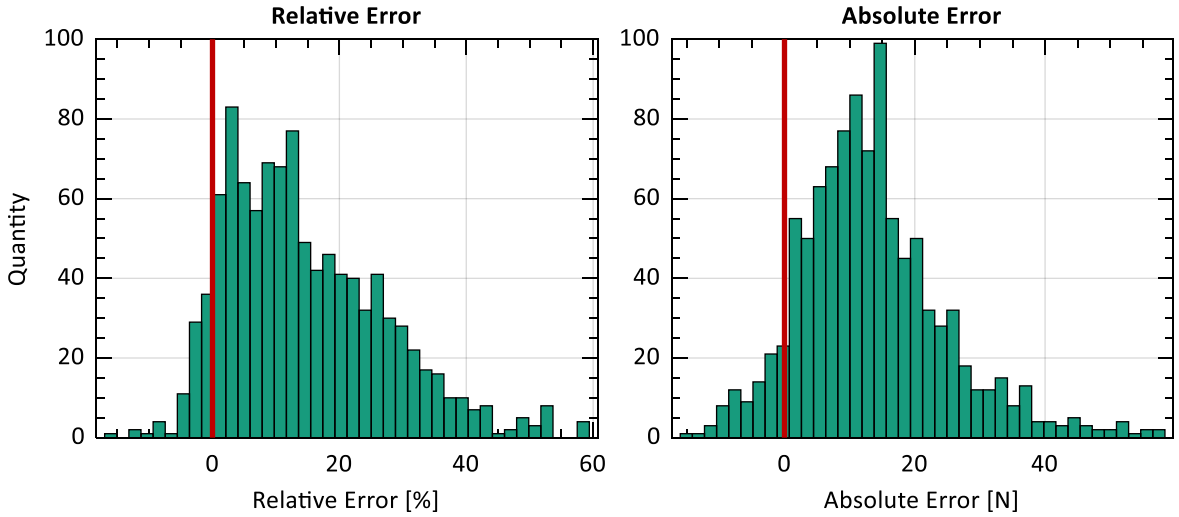

Figure 9: Comparison of measured and converted impact force for all configurations according to Table 3 (~1000 data points) using p_{app} to calculate m_R^*

7 Summary

The following example illustrates the application of the presented conversion technique and its relevance for the safety and efficiency of collaborative robots.

It is assumed that the risk assessment identified an unconstrained collision between a UR10e with 10 kg payload and the sternum (8) of the human worker as a serious risk of injury. For mitigating the risk, ISO/TS 15066 defines 280 N as the maximum force limit that the robot must not exceed in such contacts (collisions). Today, the validation of the robots ability not to exceed the limits, require to fix the PFMD during the measurement.

The impact force recorded with a fixed PFMD is given in Figure 10 for different velocities. The diagram shows that the robot complies with the force limit at a velocity of 340 mm/s (vertical yellow line). However, the fixed PFMD does not represent the conditions of a free collision, where the human body part can move into

the direction of the impact force. Therefore, RIA T R15.806-2018 suggests to use a moveable PFMD with the weight of the human body part under test ($m_H = 17.1$ kg). With such a device, the force limit is still fulfilled at a velocity of 553 mm/s, which corresponds to a velocity increase of 62% (vertical red line).

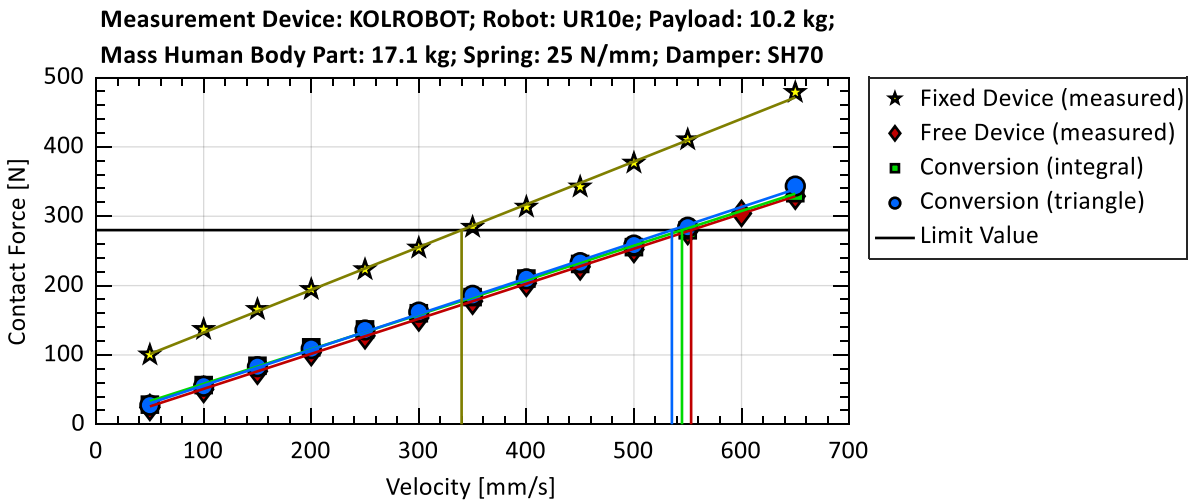

Figure 10: Results from experimental tests and obtained with both conversion techniques

Since the use of a moveable PFMD is limited to horizontal collisions and generally requires a lot of space to install it, we suggest to use the conversion technique instead. Based on the measurement from the tests with the fixed PFMD, the estimated apparent robot mass can be estimated by

$$m_R^* = \frac{v}{p} \tag{7.1}$$

where v is the programmed robot velocity and p the momentum calculated by Eq. (2.2). Then, the maximum force $\hat{F}_C$ measured in a clamping collision with the fixed PFMD can be converted into the force that would appear in a free-collision test with a moveable PFMD

$$\hat{F}_F = \hat{F}_C \sqrt{\frac{m_H}{m_H + m_R^*}} \tag{7.2}$$

by factoring in m_R^* and the mass of the human body part m_H. Figure 10 shows that this technique delivers slightly higher estimates of the maximum collision forces as measured with the moveable PFMD. Consequently, the corresponding robot velocity of 544 mm/s is slightly lower and, thus, absolutely safe (vertical green line). Although the velocity is slower, it still brings an increase of 60% compared to the velocity that was determined with the fixed PFMD.

To simplify the calculation of p, the momentum can be considered as the area of the triangle shown in Figure 8. Due to the oversimplification, the converted forces will result in slightly lower robot velocities (535 mm/s vs. 544 mm/s) as indicated by the vertical blue line.

8 Conclusion and Outlook

Within the ROSSINI project the Fraunhofer IFF developed a new technique to convert impact forces recorded with a fixed Pressure and Force Measurement Device (PFMD) into such that would occur in a free collision. The technique has been validated with three different collaborative robots and two different PFMDs. The results obtained from the simulation and experiments show a significant increase of the allowable robot velocities. The main contribution of the conversion technique to the cobot community is the opportunity to measure human-robot collisions of any direction, even in confined spaces. Both advantages outweigh the slightly lower, but more conservative allowable robot velocities that the conversion technique obtains. The finding of this study have a decisive contribution to increase the overall productivity of collaborative robots without compromising their ability to mitigate the risk of injuries to humans.

Future work will focus on the estimation of the robots velocity, which is needed to calculate the apparent mass. In fact, the translational velocity of the robot must be assumed as unknown, especially if the robot executes PTP movements or if the collision point is not at the end-effector. However, it is always possible to use the velocity threshold as it is configured in the safety controller, since safety-rated function will always ensure that the robot is never exceeding this value.

Acknowledgment

The biofidelic measurement device PRMS (PILZ Robot Measurement System) for the experiments was provided by courtesy of the project partner PILZ.

Annex: Collision test results for different configurations

UR10e with PILZ PRMS

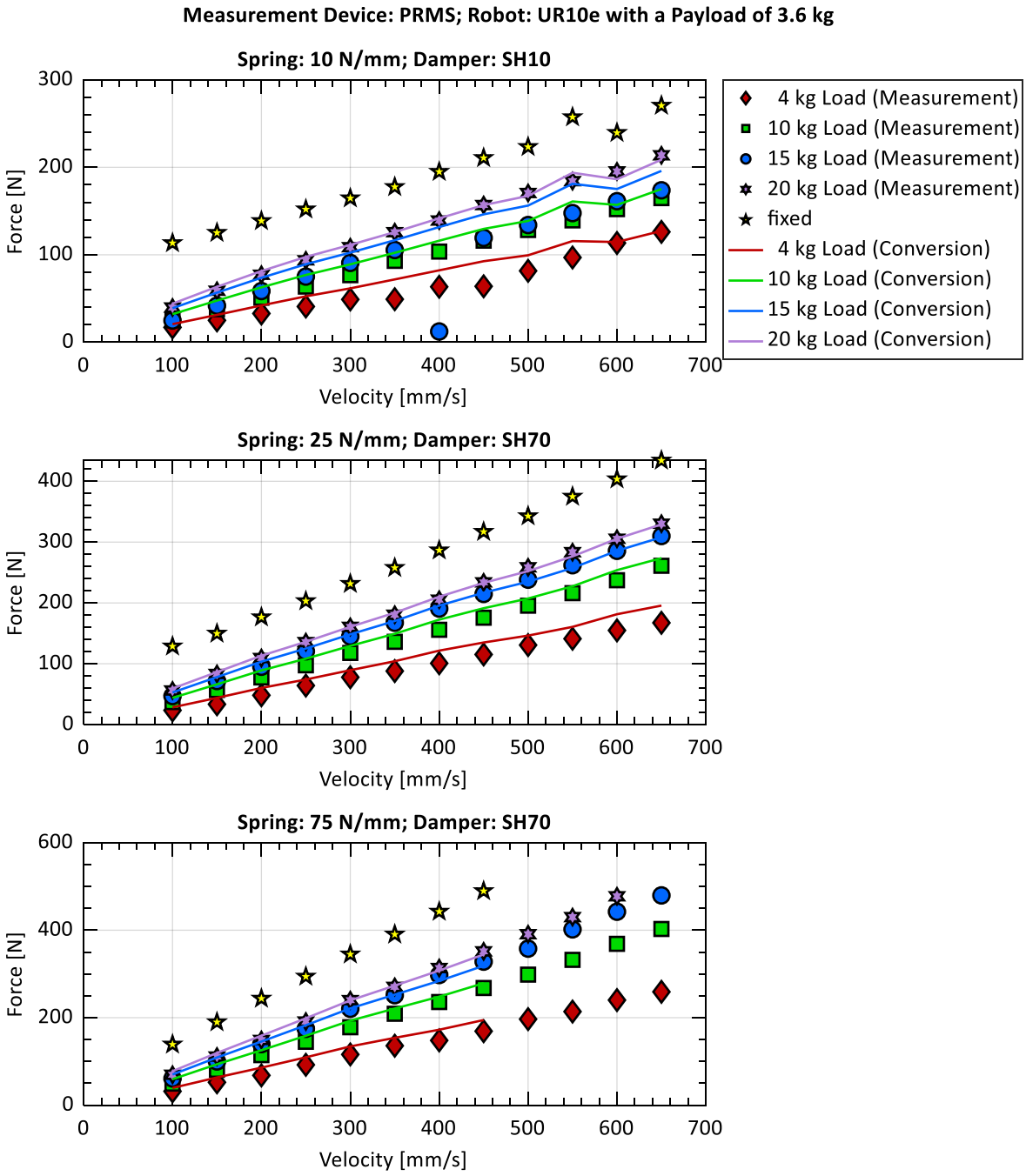

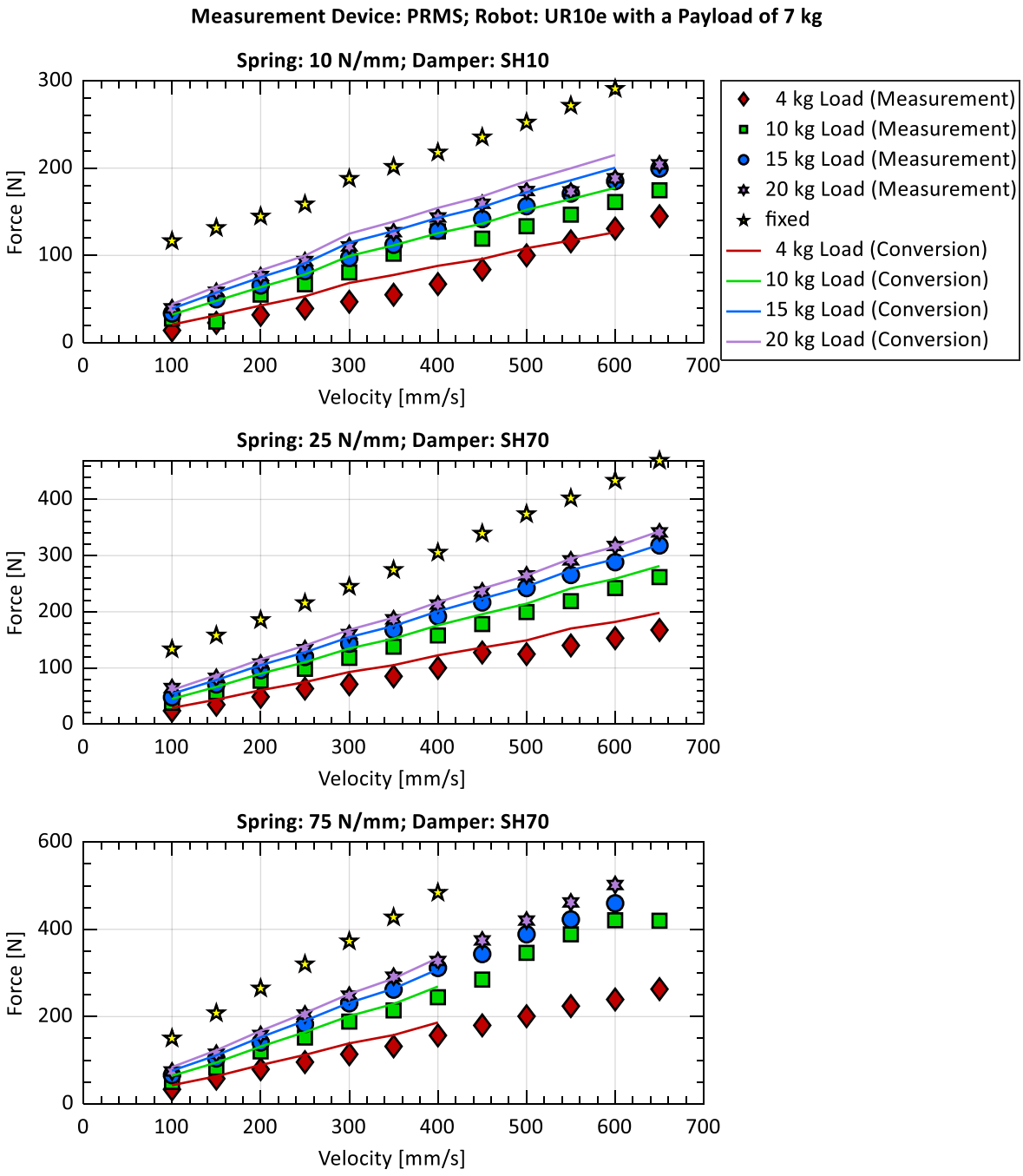
Measurement Device: PRMS; Robot: UR10e with a Payload of 7 kg
Spring: 10 N/mm; Damper: SH10
Force [N]
Velocity [mm/s]
4 kg Load (Measurement)
10 kg Load (Measurement)
15 kg Load (Measurement)
20 kg Load (Measurement)
fixed
4 kg Load (Conversion)
10 kg Load (Conversion)
15 kg Load (Conversion)
20 kg Load (Conversion)
Spring: 25 N/mm; Damper: SH70
Force [N]
Velocity [mm/s]
Spring: 75 N/mm; Damper: SH70
Force [N]
Velocity [mm/s]

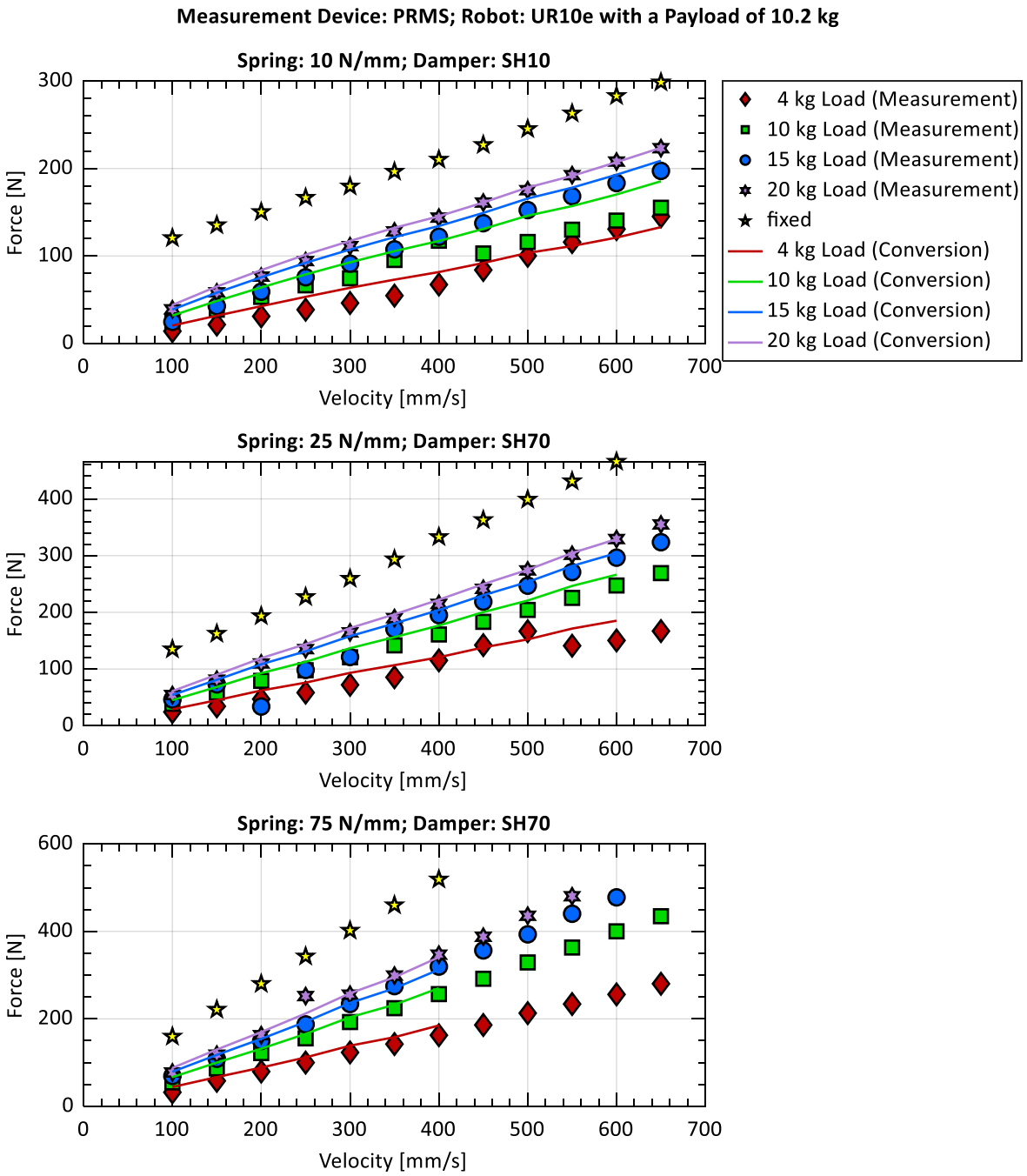
Measurement Device: PRMS; Robot: UR10e with a Payload of 10.2 kg
Spring: 10 N/mm; Damper: SH10
Force [N]
Velocity [mm/s]
4 kg Load (Measurement)
10 kg Load (Measurement)
15 kg Load (Measurement)
20 kg Load (Measurement)
fixed
4 kg Load (Conversion)
10 kg Load (Conversion)
15 kg Load (Conversion)
20 kg Load (Conversion)
Spring: 25 N/mm; Damper: SH70
Force [N]
Velocity [mm/s]
Spring: 75 N/mm; Damper: SH70
Force [N]
Velocity [mm/s]

UR10e with IFA KOLROBOT

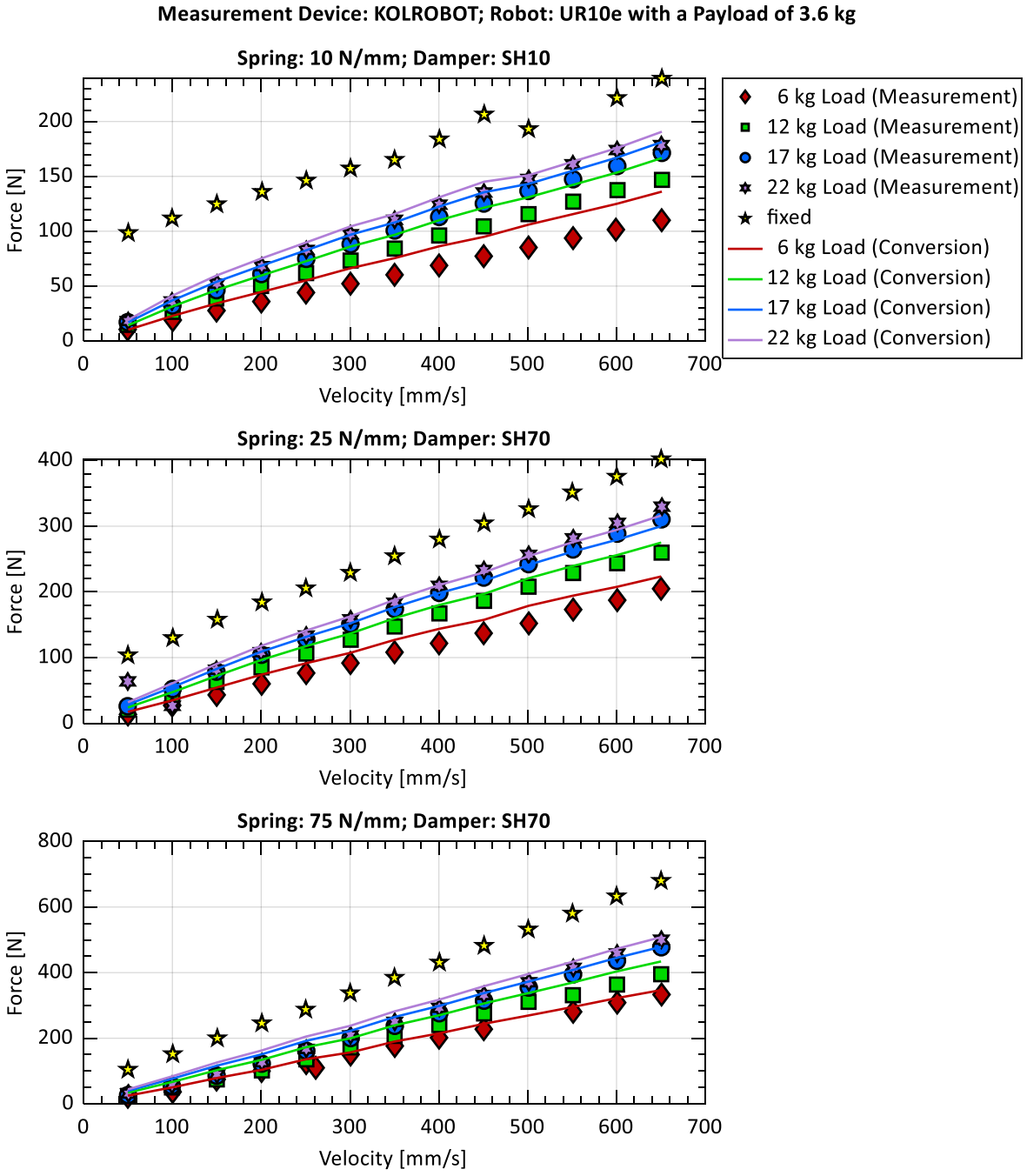

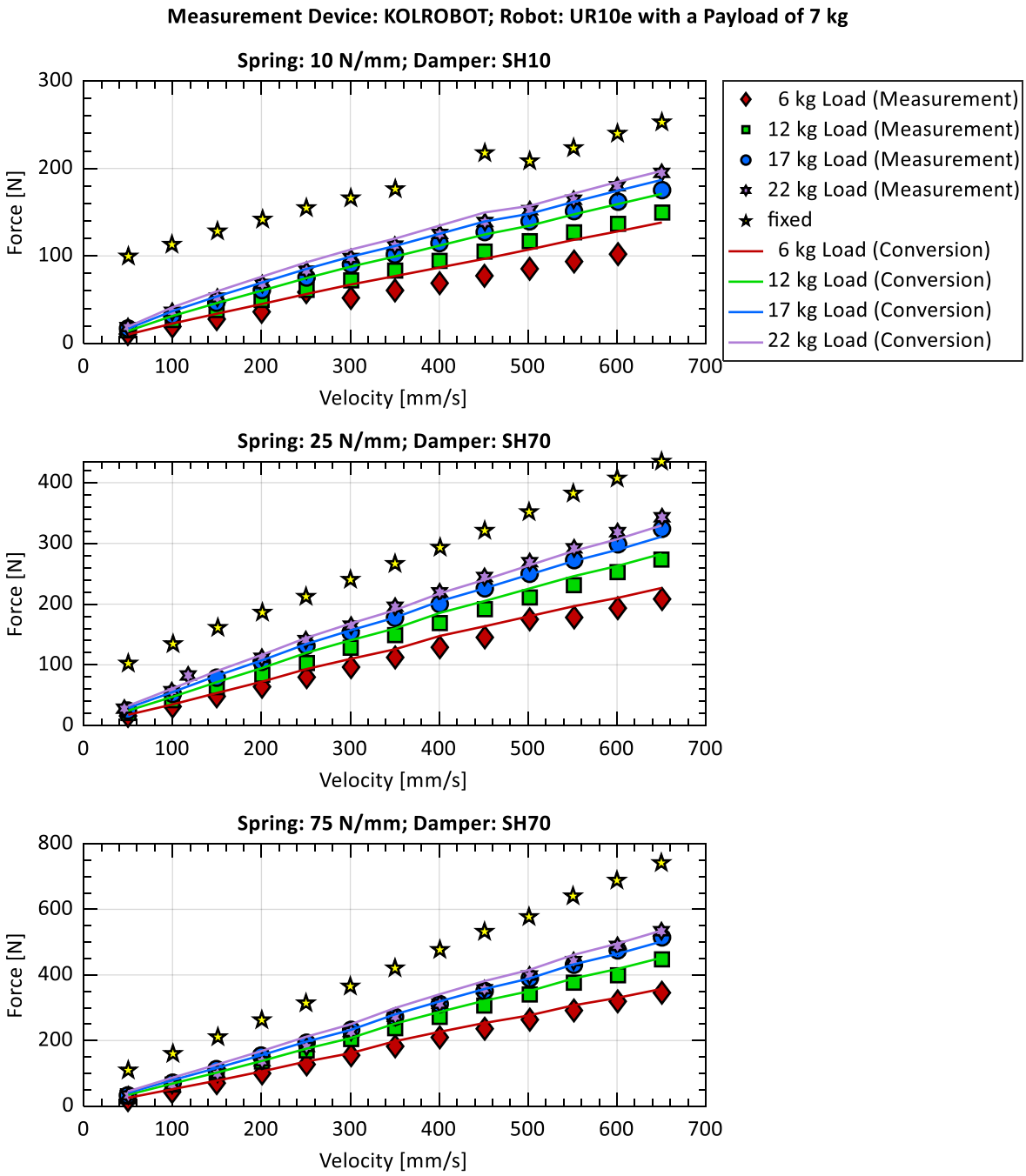
Measurement Device: KOLROBOT; Robot: UR10e with a Payload of 7 kg
Spring: 10 N/mm; Damper: SH10
Force [N]
Velocity [mm/s]
6 kg Load (Measurement)
12 kg Load (Measurement)
17 kg Load (Measurement)
22 kg Load (Measurement)
fixed
6 kg Load (Conversion)
12 kg Load (Conversion)
17 kg Load (Conversion)
22 kg Load (Conversion)
Spring: 25 N/mm; Damper: SH70
Force [N]
Velocity [mm/s]
Spring: 75 N/mm; Damper: SH70
Force [N]
Velocity [mm/s]

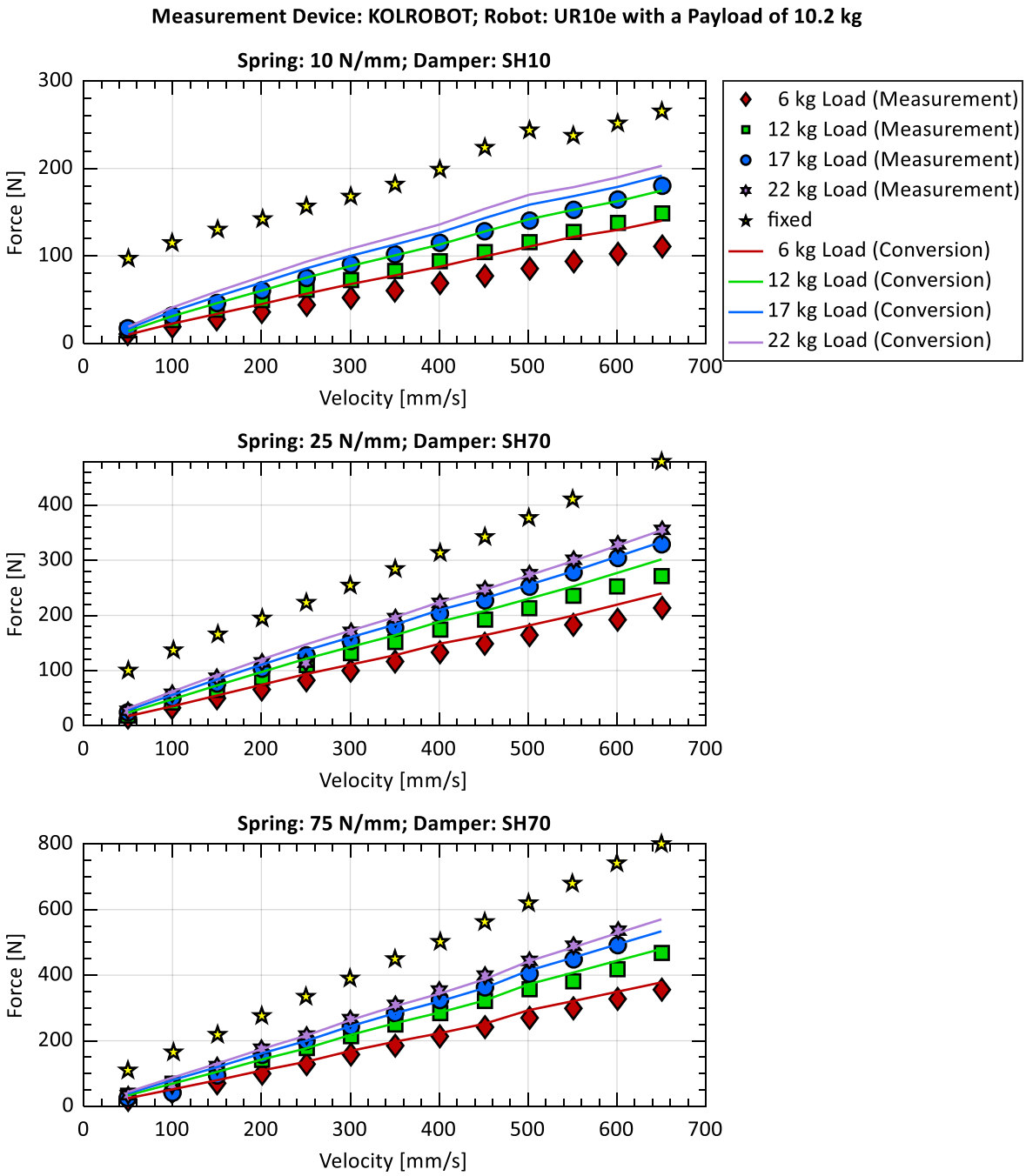
Measurement Device: KOLROBOT; Robot: UR10e with a Payload of 10.2 kg
Spring: 10 N/mm; Damper: SH10
Force [N]
Velocity [mm/s]
6 kg Load (Measurement)
12 kg Load (Measurement)
17 kg Load (Measurement)
22 kg Load (Measurement)
fixed
6 kg Load (Conversion)
12 kg Load (Conversion)
17 kg Load (Conversion)
22 kg Load (Conversion)
Spring: 25 N/mm; Damper: SH70
Force [N]
Velocity [mm/s]
Spring: 75 N/mm; Damper: SH70
Force [N]
Velocity [mm/s]

UR3e with IFA KOLROBOT

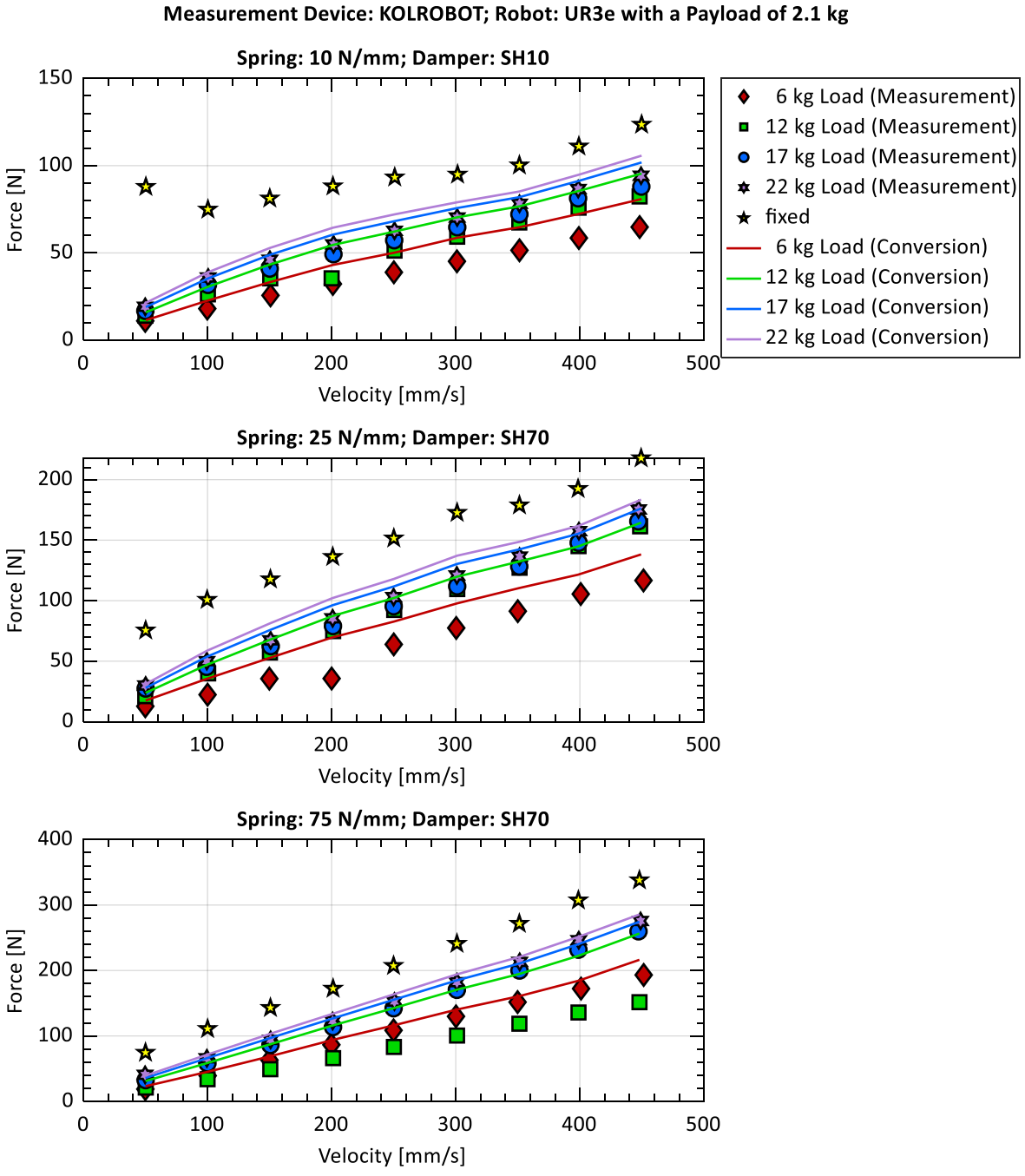

Doosan M0607 with IFA KOLROBOT

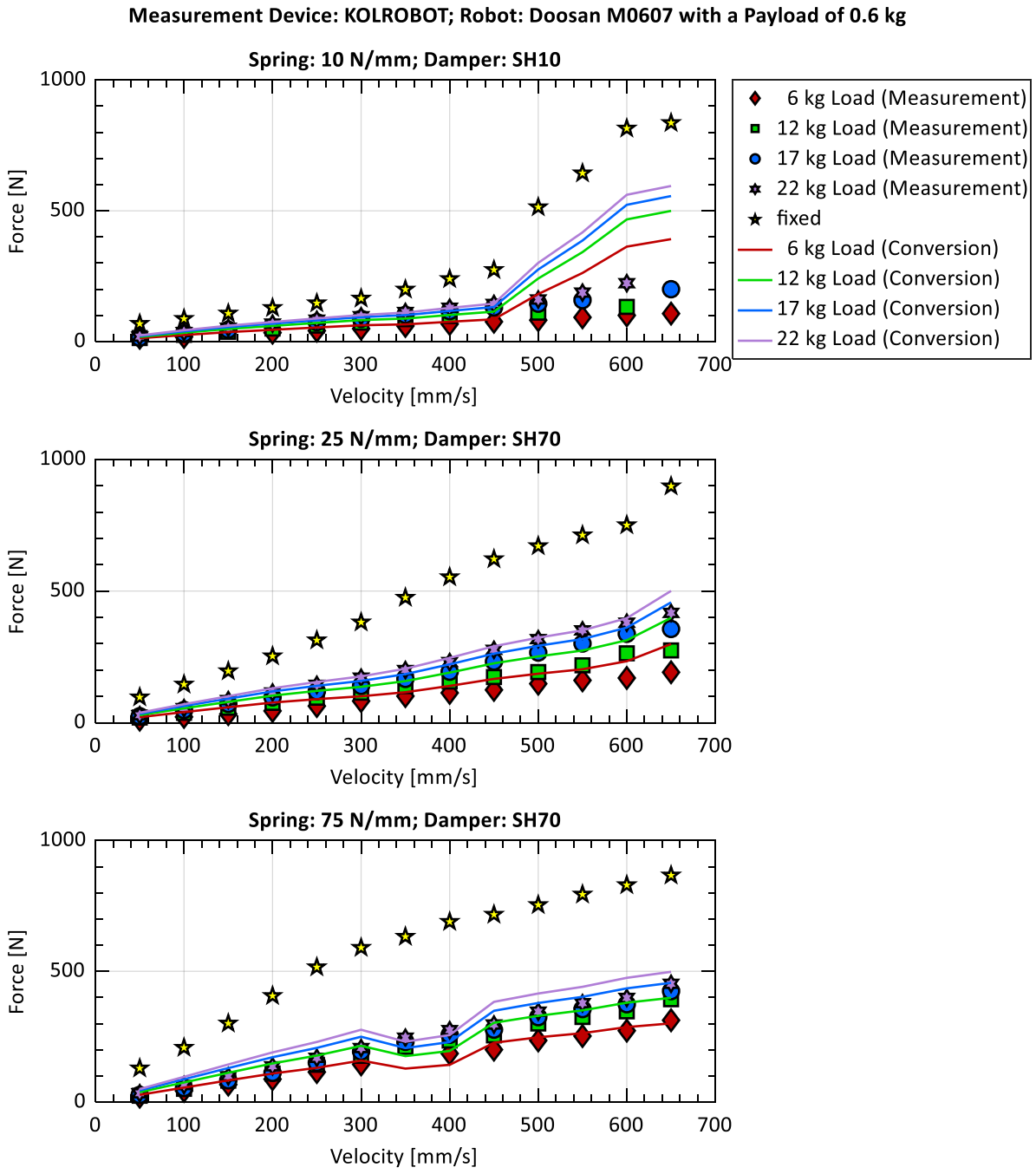

9 References

A. Albu-Schaffer; M. Fischer; G. Schreiber; F. Schoeppe; G. Hirzinger (2004): Soft robotics: what Cartesian stiffness can obtain with passively compliant, uncoupled joints? In: 2004 IEEE/RSJ International Conference on Intelligent Robots and Systems (IROS) (IEEE Cat. No.04CH37566). 2004 IEEE/RSJ International Conference on Intelligent Robots and Systems (IROS) (IEEE Cat. No.04CH37566) (4), 3295-3301 vol.4.

Behrens, R.; Saenz, J.; Vogel, C.; Elkmann, N. (2015): Upcoming Technologies and Fundamentals for Safeguarding All Forms of Human-Robot Collaboration. In: *Proceedings of the 8th International Conference on Safety of Industrial Automated Systems*.

BGHM (Hg.) (2017): DGUV-Information - Kollaborierende Robotersysteme. Planung von Anlagen mit der Funktion "Leistungs- und Kraftbegrenzung". Deutsche Gesetzliche Unfallversicherung (DGUV).

Bicchi, A.; Tonietti, G. (2004): Fast and "Soft-Arm" Tactics. In: *IEEE Robot. Automat. Mag.* 11 (2), S. 22–33. DOI: 10.1109/MRA.2004.1310939.

Falco, J.; Marvel, J.; Norcross, R. (2012): Collaborative Robotics: Measuring Blunt Force Impacts on Humans. In: Proceedings of the 7th International conference on the Safety of Industrial Automated Systems. International conference on the safety of industrial automated systems (SIAS). Montreal, Canada, October 11-12. Institut de recherche Robert-Sauvé en santé et en sécurité du travail (IRSST).

Haddadin, S.; Krieger, K.; Mansfeld, N.; Albu-Schaffer, A. (2012): On impact decoupling properties of elastic robots and time optimal velocity maximization on joint level. In: *Proceedings of 2012 IEEE/RSJ International Conference on Intelligent Robots and Systems*, S. 5089–5096. DOI: 10.1109/IROS.2012.6385913.

Huelke, M.; Ottersbach, H.-J. (2012): How to approve Collaborating Robots. The IFA force pressure measurement system. In: Proceedings of the 7th International conference on the Safety of Industrial Automated Systems, Bd. 7. International conference on the safety of industrial automated systems (SIAS). Montreal, Canada, October 11-12. Institut de recherche Robert-Sauvé en santé et en sécurité du travail (IRSST).

Khatib, O. (1987): A unified approach for motion and force control of robot manipulators: The operational space formulation. In: *IEEE Journal on Robotics and Automation* 3 (1), S. 43–53. DOI: 10.1109/JRA.1987.1087068.

Khatib, O. (1995): Inertial Properties in Robotic Manipulation: An Object-Level Framework. In: *The International Journal of Robotics Research* 14 (1), S. 19–36. DOI: 10.1177/027836499501400103.

Oberer-Treitz, S. (2017): Abschätzung der Kollisionsfolgen von Robotern zur Bewertung des sicheren Einsatzes in der Mensch-Roboter-Kooperation. Dissertation. Universität Stuttgart. Institut für Steuerungstechnik der Werkzeugmaschinen und Fertigungseinrichtungen (ISW). Online verfügbar unter http://elib.uni-stuttgart.de/bitstream/11682/9715/1/Oberer-Treitz_77_.pdf.

Zinn, M.; Roth, B.; Khatib, O.; Salisbury, J. K. (2004): A new actuation approach for human friendly robot design. In: *The International Journal of Robotics Research*. Online verfügbar unter http://worldcatlibraries.org/wcpa/oclc/926326925.